Research Article

FLOW MODELING AND DESIGN OF MR FLUID DAMPER FOR VIBRATION SUPPRESSION

Sailaja G

Department of Mech. Engineering., MJCET, Road No.3, Banjara Hills, Hyderabad-34

ARTICLE INFO	ABSTRACT
	Magnetorheological (MR) fluids are the fluids that respond to an applied magnetic field with a vivid change in rheological behavior. An MR fluid is a free-flowing liquid in the absence of magnetic field, but under a strong magnetic field its viscosity can be increased by more than two orders of magnitude in a very short time (milliseconds) and it exhibits solid-like characteristics. The strength of an MR fluid can be described by shear yield stress. Moreover, the change in viscosity is continuous and reversible, i.e. after removing the magnetic field the MR fluid can revert to a free flowing liquid. This paper describe two quasi-static models, a parallel-plate model and an axisymmetric model, based on the Navier-Stokes equation are developed for MR damper behavior. The Herschel-Bulkley visco-plasticity model is employed to describe the MR fluid field dependent characteristics and shear thinning/thickening effects. Simple equations based on these damper models are given which can be used in the initial design phase. Effects of geometry on MR damper performance, controllable force and dynamic range, are also discussed. Also, describe the complete design and some practical design considerations for developing and testing small capacity prototype MR fluid linear vibration damper. In design process we come across geometry design to choose an appropriate gap size`g' and active pole length`L' such that the design requirements of dynamic range and controllable force are achieved. Tasks in the design of a magnetic circuit are to determine necessary amp-turns (NI) for the magnetic circuit.

INTRODUCTION

Magnetorheological (MR) fluids are the suspensions of micron sized, magnetisable particles (iron, iron oxide, iron nitride, iron carbide, carbonyl iron, chromium dioxide, low-carbon steel, silicon steel, nickel, cobalt, and combinations thereof [1]) in an appropriate carrier liquid (non-magnetisable) such as mineral oil, synthetic oil, water or ethylene glycol. The carrier liquid serves as a dispersed medium and ensures the homogeneity of particles in the fluid. A typical MR fluid consists of 20-40 percent by volume of relatively pure, 3-10 micron diameter iron particles, suspended in a carrier liquid [2]. They are field responsive in nature and the Magnetorheological response of these fluids lies in the fact that the polarization is induced in the suspended particles by the application of an external magnetic field. This allows the fluid to transform from freely flowing liquid state to solid-like state within milliseconds, because the magnetically dispersed particles attract each other to form fibril/chain-like structures along the direction of magnetic field. The chain-like structures resist the motion of the fluid and increase its viscous characteristics. Such behavior of MR fluid

is analogous to Bingham plastics (non-Newtonian fluids) capable of developing a yield stress [3]. Fig.1 shows the synthesized MR fluid (Carrier fluid- Silicone Oil and Magnetisable particles-Carbonyl Iron of around 8 microns) for 40% by volume concentration of iron particles inclusive of additives [4].

Fig 1 MR Fluid (Courtesy, MJCET)

A Favorable arrangement consists of particle chains aligned in the direction of the applied field and this, in turn, gives rise to a strong resistance to applied strains (Fig.2).

Corresponding author: **Sailaja G**
Department of Mech. Engineering., MJCET, Road No.3, Banjara Hills, Hyderabad-34
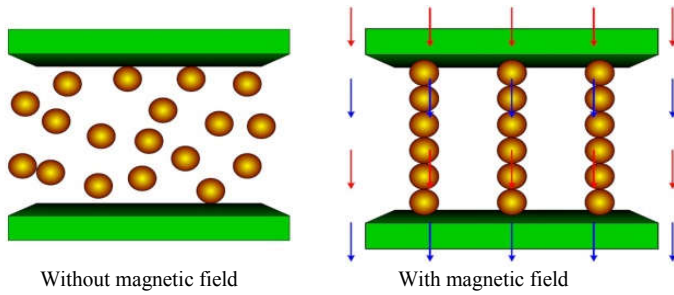
Without magnetic field   With magnetic field

Fig 2 Activation of MR fluid (Courtesy, Lord Corporation, USA)

The yield stress developed within the MR fluid is a function of the applied magnetic field. However, once this yield stress is exceeded, the behavior of the MR fluid deviates from that of a Bingham plastic. This is attributable to the breakdown of the chains of particles under the forces of the fluid flow, and results in a shear-stress/shear-rate characteristic that is highly non-linear. When used in a damping device, the result is a damper whose force/velocity characteristic is non-linear, but can be changed by the way the magnetic field is applied [5].

Having great potential for engineering applications due to their variable rheological behavior, MR fluids find applications in dampers, brakes, shock absorbers, suspensions, clutches and engine mounts.

MR Fluid Flow in an Annular Duct

The pressure gradient along the flow is resisted by the fluid shear stress which is governed by the Navier- Stokes equation

$$\rho \frac{\partial}{\partial t} u_x(r) + \frac{\partial}{\partial r} \tau_{xr}(r) + \frac{\tau_{xr}(r)}{r} = \frac{\partial p}{\partial x} \qquad (1)$$

where $u_x(r)$ = flow velocity; $\tau_{xr}(r)$ = shear stress; r = radial coordinate; x = longitudinal coordinate; ρ = fluid density; and $\partial p / \partial x$ = pressure gradient.

To analyze the quasi-static motion of the fluid inside the damper, the fluid inertial can be neglected [6]. In this case, Eq. (1) can be reduced to

$$\frac{d}{dr} \tau_{xr}(r) + \frac{\tau_{xr}(r)}{r} = \frac{dp}{dx} \qquad (2)$$

Note that for oscillatory or unsteady flow, the fluid inertia must be taken into account. The solution of Eq. (2) is

$$\tau_{rx}(r) = \frac{1}{2} \frac{dp(x)}{dx} r + \frac{D_1}{r} \qquad (3)$$

Where D_1 = a constant which can be evaluated with boundary conditions.

A typical shear stress diagram, along with velocity profile, for MR fluid flow through the annular gap is shown in Fig.3. In regions I and II, the shear stress has exceeded the yield stress and fluids flow. In region C, because the shears stress is less than the yield stress, there is no shear flow; this is often referred to as the plug flow region.

Modeling Based on the Herschel-Bulkley Model

To account for the fluid shear thinning or thickening effect, the Herschel-Bulkley visco-plasticity model is employed. In region I, the shear strain rate $\dot{\gamma} = du_x/dr \geq 0$. Therefore, the shear stress given by

$$\tau_{rx}(r) = \tau_\circ(r) + K \left(\frac{du_x(r)}{dr} \right)^{\frac{1}{m}} \qquad (4)$$
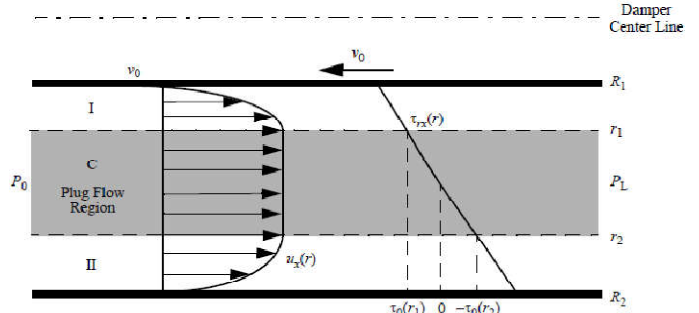

Fig 3 Stress and velocity profiles of MR fluids through an annular duct.

This is substituted into Eq. (3) and integrated once with respect to r. One obtains

$$u_x(r) = \int_{R_1}^{r} \left[\frac{1}{K} \left(\frac{1}{2} \frac{dp(x)}{dx} r + \frac{D_1}{r} - \tau_\circ(r) \right) \right]^m dr - v_p$$

$$(R_1 \leq r \leq r_1) \qquad (5)$$

by imposing the boundary condition that the flow velocity at $r = R_1$ is $u_x(R_1) = -v_p$.

In region II, the shear strain rate $\dot{\gamma} = du_x/dr \leq 0$. Thus, the shear stress is given by

$$\tau_{rx}(r) = -\tau_\circ(r) - K \left(\frac{-du_x(r)}{dr} \right)^{\frac{1}{m}} \qquad (6)$$

Similarly proceeding in region II with the boundary condition $u_x(R_2) = 0$ at r = R_2 gives

$$u_x(r) = \int_{r}^{R_2} \left[-\frac{1}{k} \left(\frac{1}{2} \frac{dp(x)}{dx} r + \frac{D_1}{r} + \tau_0(r) \right) \right]^m dr$$

$$(r_2 \leq r \leq R_2) \qquad (7)$$

Note that the flow velocity is constant in the plug flow region because the shear stress is less than the yield stress. Thus, the flow velocities at the boundaries of the plug flow region satisfy $u_x(r_1) = u_x(r_2)$. Combining Eqs. (5) and (8) yields

$$\int_{R_1}^{r_1} \left[\frac{1}{K} \left(\frac{1}{2} \frac{dp(x)}{dx} r + \frac{D_1}{r} - \tau_0(r) \right) \right]^m dr -$$

$$\int_{r_2}^{R_2} \left[-\frac{1}{K} \left(\frac{1}{2} \frac{dp(x)}{dx} r + \frac{D_1}{r} + \tau_0(r) \right) \right]^m dr = v_p \qquad (8)$$

Also the shear stresses τ_{rx} satisfy $\tau_{rx}(r_1)=\tau_0(r_1)$ and $\tau_{rx}(r_2)=-\tau_o(r_2)$, therefore D_1 can be determined by using Eq. (3) as

$$D_1=\frac{r_1 r_2\left(\tau_0(r_2)r_1+\tau_0(r_1)r_2\right)}{r_2{}^2-r_1{}^2} \tag{9}$$

The expression for the volume flow rate Q given by

$$Q=2\pi\int_{R_1}^{R_2}ru_x(r)dr \tag{10}$$

Because the shear strain rate $du_x(r)/dr$ is zero in the plug flow region $r_1<r<r_2$, Eq. (10) can also be written as

$$Q=v_p A_p=\pi R_1{}^2 v_p-\pi\int_{R_1}^{r_1}r^2\frac{du_x(r)}{dr}dr-\pi\int_{r_2}^{R_2}r^2\frac{du_x(r)}{dr}dr \tag{11}$$

Where $A_P=$ Cross section area of the piston head, and $v_p=$ piston head velocity. Substitution of Eqs. (5) and (7) into Eq. (11) results in

$$Q=v_p A_p=\pi R_1{}^2 v_p-\pi\int_{R_1}^{r_1}r^2\left[\frac{1}{K}\left(\frac{1}{2}\frac{dp(x)}{dx}r+\frac{D_1}{r}-\tau_o(r)\right)\right]^m dr$$
$$+\pi\int_{r_2}^{R_2}r^2\left[-\frac{1}{K}\left(\frac{1}{2}\frac{dp(x)}{dx}r+\frac{D_1}{r}+\tau_0(r)\right)\right]^m dr \tag{12}$$

Fig. 4 shows the free body diagram of MR fluids through an annular duct. The equation of motion of fluid materials enclosed by $r=r_1$ and $r=r_2$ is

$$\frac{dp}{dx}\pi\left(r_2{}^2-r_1{}^2\right)dx+2\pi r_2\tau_0(r_2)dx+2\pi r_1\tau_0(r_1)dx=0 \tag{13}$$
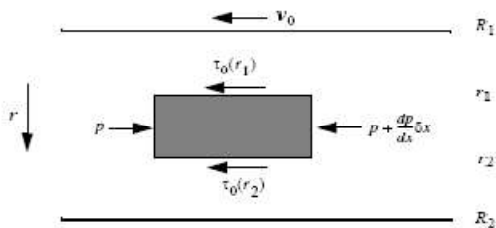
which yields

Fig 4 Free body diagram of MR fluids through an annular duct

$$\frac{dp(x)}{dx}\left(r_2{}^2-r_1{}^2\right)+2\left[\tau_0(r_2)r_2+\tau_0(r_1)r_1\right]=0 \tag{14}$$

In summary, the resulting equations that can be solved numerically to determine r_1, r_2, and the pressure gradient $\frac{dp}{dx}$ between the two ends of the cylinder using the Herschel-Bulkley model are given by

$$\int_{R_1}^{r_1}\left[\frac{1}{K}\left(\frac{1}{2}\frac{dp(x)}{dx}r+\frac{D_1}{r}-\tau_o(r)\right)\right]^m dr-\int_{r_2}^{R_2}\left[-\frac{1}{K}\left(\frac{1}{2}\frac{dp(x)}{dx}r+\frac{D_1}{r}+\tau_0(r)\right)\right]^m dr=v_p \tag{15}$$

$$Q=v_p A_p=\pi R_1{}^2 v_p-\pi\int_{R_1}^{r_1}r^2\left[\frac{1}{K}\left(\frac{1}{2}\frac{dp(x)}{dx}r+\frac{D_1}{r}-\tau_o(r)\right)\right]^m dr$$
$$+\pi\int_{r_2}^{R_2}r^2\left[-\frac{1}{K}\left(\frac{1}{2}\frac{dp(x)}{dx}r+\frac{D_1}{r}+\tau_0(r)\right)\right]^m dr \tag{16}$$

$$\frac{dp(x)}{dx}\left(r_2{}^2-r_1{}^2\right)+2\left[\tau_0(r_2)r_2+\tau_0(r_1)r_1\right]=0 \tag{17}$$

Where $D_1=\frac{r_1 r_2\left[\tau_0(r_2)r_1+\tau_0(r_1)r_2\right]}{r_2{}^2-r_1{}^2}$ (18)

To solve the resulting algebraic equations numerically, a method based on the constrained nonlinear least-squares algorithm is utilized in conjunction with the cubic polynomial interpolation and extrapolation method. The integrals in Eqs. (15) and (16) are evaluated using the adaptive recursive Newton-Cotes approach.

From Eq. (17) the thickness of the plug flow region can be obtained by

$$r_2-r_1=-\frac{2\left[\tau_0(r_1)r_1+\tau_0(r_2)r_2\right]}{\dfrac{dp(x)}{dx}(r_1+r_2)} \tag{19}$$

which varies with the fluid yield stress τ_0. Note that the flow can only be established when $r_2-r_1<R_2-R_1$, which implies that the plug flow needs to be within the gap otherwise, there is no flow.

The damper force is then computed as

$$F=\Delta p A_p \tag{20}$$

where $\Delta P=P_L-P_o=-L\left(dp(x)/dx\right)$; and $L=$ effective pole length. The velocity profile can be determined from Eqs. (5) and (7) as follows:

$$u_x(r)=\int_{R_1}^{r}\left[\frac{1}{k}\left(\frac{1}{2}\frac{dp(x)}{dx}r+\frac{D_1}{r}-\tau_0(r)\right)\right]^m dr-v_p \quad R_1\le r\le r_1$$

$$u_x(r)=\int_{r_2}^{R_2}\left[-\frac{1}{k}\left(\frac{1}{2}\frac{dp(x)}{dx}r+\frac{D_1}{r}+\tau_0(r)\right)\right]^m dr \quad r_1<r<r_2 \tag{21}$$

$$u_x(r)=\int_{r}^{R_2}\left[-\frac{1}{k}\left(\frac{1}{2}\frac{dp(x)}{dx}r+\frac{D_1}{r}+\tau_0(r)\right)\right]^m dr \quad r_2\le r\le R_2$$

Further, the shear stress diagram can be obtained from Eq. (3) Note that when the yield stress $\tau_0=0$, there is no plug flow region which implies that $r_1=r_2$. Therefore, Eqs. (17) and (18) are no longer valid due to the singularity. However, in this case, the velocity achieves its maximum at $r=r_1$ where the shear stress is zero. By using Eq. (3), the following equations can be employed to obtain pressure gradient where yield stress $\tau_0=0$

$$\int_{R_1}^{r_1}\left[\frac{1}{K}\left(\frac{1}{2}\frac{dp(x)}{dx}r+\frac{D_1}{r}\right)\right]^m dr-\int_{r_1}^{R_2}\left[-\frac{1}{K}\left(\frac{1}{2}\frac{dp(x)}{dx}r+\frac{D_1}{r}\right)\right]^m dr=v_p \tag{22}$$

$$Q=v_p A_p=\pi R_1{}^2 v_p-\pi\int_{R_1}^{r_1}r^2\left[\frac{1}{K}\left(\frac{1}{2}\frac{dp(x)}{dx}r+\frac{D_1}{r}\right)\right]^m dr$$
$$+\pi\int_{r_1}^{R_2}r^2\left[-\frac{1}{K}\left(\frac{1}{2}\frac{dp(x)}{dx}r+\frac{D_1}{r}\right)\right]^m dr \tag{23}$$

$$D_1 = \frac{1}{2}\frac{dp}{dx}r_1^2 \tag{24}$$

Note that the solution of the MR flow in an annular duct does not reduce to that of the pipe flow as $r_1 \rightarrow 0$. This is because the annular duct model has a boundary condition at r_1; however, there is no boundary condition at r = 0 for the pipe flow.

Modeling based on the Bingham model

The Herschel-Bulkley model reduces to the Bingham model when the MR fluid parameter m =1. Using Eqs. (15) − (17), the resulting equations for the Bingham model are

$$\frac{dp(x)}{dx}\left(R_2^2 - r_2^2 - R_1^2 + r_1^2\right)/4 + D_1 \ln\left(R_2 r_1 / r_2 R_1\right) + D_2 - \eta v_p = 0 \tag{25}$$

$$Q = v_p A_p$$
$$= \pi R_1^2 v_p - \frac{\pi}{8\eta}\left[\frac{dp(x)}{dx}\left(R_2^4 - R_1^4 - r_2^4 + r_1^4\right) + 4D_1\left(R_2^2 - R_1^2 - r_2^2 + r_1^2\right) + 8D_3\right] \tag{26}$$

$$\frac{dp(x)}{dx}\left(r_2^2 - r_1^2\right) + 2\left[\tau_0(r_2)r_2 + \tau_0(r_1)r_1\right] = 0 \tag{27}$$

where
$$D_1 = \frac{r_1 r_2\left[\tau_0(r_2)r_1 + \tau_0(r_1)r_2\right]}{r_2^2 - r_1^2} \tag{28}$$

$$D_2 = \int_{r_2}^{R_2}\tau_0(r)dr + \int_{r_1}^{R_1}\tau_0(r)dr \tag{29}$$

$$D_3 = \int_{r_2}^{R_2}\tau_0(r)r^2 dr + \int_{r_1}^{R_1}\tau_0(r)r^2 dr \tag{30}$$

and the velocity profile is given by

$$u_x(r) = \frac{-1}{4\eta}\frac{dp}{dx}\left(R_1^2 - r^2\right) + \frac{D_1}{\eta}\ln\frac{r}{R_1} - \frac{1}{\eta}\int_{R_1}^{r}\tau_0(r)dr - v_p \quad R_1 \leq r \leq r_1$$
$$= \frac{-1}{4\eta}\frac{dp}{dx}\left(R_2^2 - r_2^2\right) - \frac{D_1}{\eta}\ln\frac{R_2}{r_2} - \frac{1}{\eta}\int_{r_2}^{R_2}\tau_0(r)dr \quad r_1 < r < r_2 \tag{31}$$
$$= \frac{-1}{4\eta}\frac{dp}{dx}\left(R_2^2 - r^2\right) - \frac{D_1}{\eta}\ln\frac{R_2}{r} - \frac{1}{\eta}\int_{r}^{R_2}\tau_0(r)dr \quad r_2 \leq r \leq R_2$$

In the absence of magnetic field, the yield stress $\tau_0 = 0$. The pressure gradient can be obtained directly from

$$\frac{dp}{dx} = \frac{8\eta v_p}{\pi}\frac{\frac{\pi}{2}(2R_1^2 - \frac{R_2^2 - R_1^2}{\ln(R_2/R_1)}) - A_P}{R_2^4 - R_1^4 - \frac{(R_2^2 - R_1^2)^2}{\ln(R_2/R_1)}} \tag{32}$$

In general, the yield stress τ_0 in the axisymmetric model will be a function of r. But when $R_2 - R_1 << R_1$, variation of the yield stress in the gap can be ignored, and Eqs. (28)− (30) can be further simplified substantially as follows:

$$D_1 = \frac{r_1 r_2 \tau_0}{r_2 - r_1} \tag{33}$$

$$D_2 = \tau_0\left(R_2 + R_1 - r_1 - r_2\right) \tag{34}$$

$$D_3 = \frac{1}{3}\tau_0\left(R_1^3 + R_2^3 - r_1^3 - r_2^3\right) \tag{35}$$

Note that in this case, the thickness of the plug flow can be calculated by using Eq. (19) $r_2 - r_1 = -\dfrac{2\tau_0}{\dfrac{dp(x)}{dx}}$ (36)

Which is a constant, and only depends on the yield stress and pressure gradient of the flow.

MR Damper Design

The design process consists of two stages i.e. Geometry design and Magnetic circuit design which are explained in the following sections.

MR Damper Geometry Design

Most devices that use MR fluids can be classified as having either fixed poles (pressure driven flow mode) or relatively moveable poles (direct-shear mode). Diagrams of these two basic operational modes are shown in Fig.5.

A third mode of operation known as squeeze-film mode has also been used in low motion, high force applications.

The MR fluid damper devices operate in pressure driven flow mode (PDF). During motion of the MR damper piston, fluids flow in the annular gap between the piston and the cylinder housing. For quasi-static analysis of MR fluid dampers, assume that: 1) MR dampers move at a constant velocity; 2) MR fluid flow is fully developed; 3) a simple Bingham plasticity model may be employed to describe the MR fluid behavior.
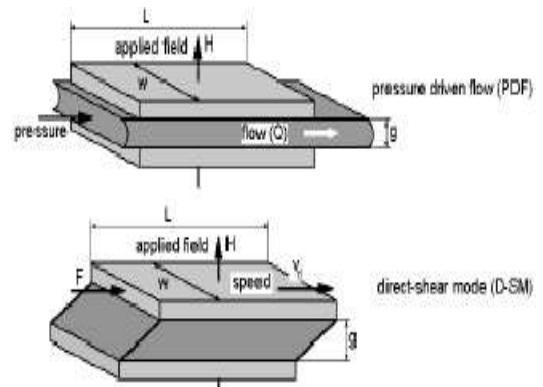

Fig 5 Basic operational modes for controllable fluid devices

Conform the Bingham plasticity model the flow is governed by (Bingham's equations):

$$\tau = G \cdot \gamma, \qquad \tau < \tau_y$$
$$\tau = \tau_y(H) + \eta \cdot \gamma^\bullet, \qquad \tau > \tau_y. \tag{37}$$

(in the absence of magnetic field $\tau \approx \eta \cdot \gamma^\bullet$).

In Eq. (1), H is the magnetic field, $\gamma^\bullet$ is the fluid shear rate, η is the plastic viscosity (i.e. viscosity at H=0), and G is the complex material modulus.

Fig.3 provides a typical shear stress diagram and velocity profile of the Bingham plastic shear flow in the annular gap. In regions I and II, the shear stress has exceeded the yield stress; therefore, the fluid flows. In region C, the shear stress is lower than the yield stress, so no shear flow occurs; this is often referred to as the plug flow region.

In an analogous fashion to Eqs. (37), the pressure drop developed in a device based on pressure driven flow mode is commonly assumed to result from the sum of a viscous component ΔP_η and a field dependent induced yield stress component ΔP_τ. This pressure may be approximated by:

$$\Delta P = \Delta P_\eta + \Delta P_\tau = \frac{12 \cdot \eta \cdot Q \cdot L}{g^3 \cdot w} + \frac{c \cdot \tau_y \cdot L}{g} \qquad (38)$$

Where L, g and w are the length, gap and width of the flow channel between the fixed poles, Q is the volumetric flow rate, η is the fluid viscosity with no applied field and τ_y is the yield stress developed in response to an applied field. The parametric c has a value ranging from a minimum value of 2 (for $\lambda < 1$) to a maximum value of 3 (for $\lambda > 100$). Where λ is control ratio or dynamic range ($\lambda = \Delta P_\tau / \Delta P_\eta$).

The volume of MR fluid exposed to the magnetic field and thus is responsible in providing the desired MR effect is named the minimum active volume V:

$$V = k \cdot \left(\frac{\eta}{\tau^2} \right) \cdot \lambda \cdot W_m \qquad (39)$$

Where k=12/c² is a constant and V=L·w·g can be regarded as the necessary active fluid volume in order to achieve the desired control ratio λ at a required controllable mechanical power level W_m ($W_m = Q \cdot \Delta P_\tau$).

By noting V=L·w·g, and $W_m = Q \cdot \Delta P_\tau$, Eq. (39) can be further manipulated to give: $w \cdot g^2 = \frac{12}{c} \cdot \left(\frac{\eta}{\tau_y} \right) \cdot \lambda \cdot Q$ (40)

This equation provides geometric constrains and the necessary aspect ratios for MR devices based on MR fluid properties, the desired control ratio or dynamic range, and the device flow (or speed).

MR fluid devices are usually designed such that MR fluid can be, or nearly can be, magnetically saturated. It is under this condition that the fluid will generate its maximum yield stress τ_y. However, the value τ_y that is used in the above equations should be chosen from the MR fluid specification sheets to reflect the anticipated operating condition.

Based on the operational model for pressure driven flow, plotted in Fig.5, is possible to determine the effect of geometry on MR damper performance, controllable force and dynamic range D.

As illustrated in Fig.6, the damper resisting force can be decomposed into a controllable force F_τ due to controllable yield stress τ_y and uncontrollable force F_{uc}. The uncontrollable force includes a viscous force F_η and a friction force F_f. By definition, the dynamic range is the ratio between the total damper output force F and the uncontrollable force F_{uc}:

$$D = 1 + \frac{F_\tau}{F_\eta + F_f} \qquad (41)$$

Where $F_\eta = \left(A_p . v_p + \frac{w \cdot g \cdot v_p}{2} \right) \cdot \frac{12 \cdot \eta \cdot L \cdot A_p}{w \cdot g^3}$ (42)

$$F_\tau = \frac{c \cdot \tau_y \cdot L \cdot A_p}{g} \cdot sgn(v_p) \qquad (43)$$

In Eq. (43) parameter c is bounded to the interval [2.07, 3.07].

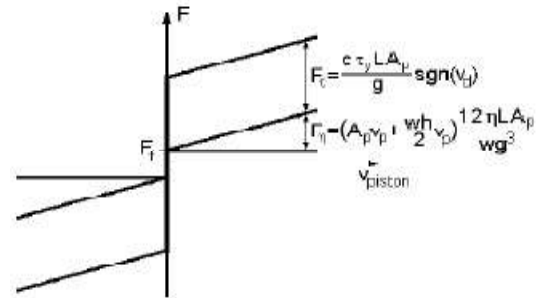The controllable force [Eq. (43)] can be rewritten:

Fig 6 Force decomposition of MR dampers

$$F_\tau = \left(2.07 + \frac{12 \cdot Q \cdot \eta}{12 \cdot Q \cdot \eta + 0.4 \cdot w \cdot g^2 \cdot \tau_y} \right) \cdot \frac{\tau_y \cdot L \cdot A_p}{g} \cdot sgn(v_p)$$

which indicates that the controllable force range is inversely related to the gap size g. To maximize the effectiveness of MR damper, the controllable force should be as large as possible; therefore, a small gap size is required. However, a small gap size decreases the dynamic range.

The expression of dynamic range D in Eq. (41) can be rewritten using Eqs. (42) and (43):

$$D = 1 + \frac{c \cdot \tau_y \cdot L \cdot A_p}{\left(A_p + \frac{w \cdot g}{2} \right) \cdot \frac{12 \cdot \eta \cdot L \cdot A_p \cdot v_p}{w \cdot g^2} + g \cdot F_f} \qquad (44)$$

At Institute of solid mechanics, the quasi-static model developed previously has been useful for designing a new MR fluid damper for experimental study.

The given data for prototype MR fluid damper are:

- Controllable mechanical power level $W_m = 200W$;

- Maximum piston speed $v_p^{max} = 0.2$ m/s;

- Minimum piston speed $v_p^{min} = 0.05$ m/s;

- Stroke $= \pm 0.03$ m;

- Inside diameter of cylinder $d_{cyl} = 0.04$ m;

- Piston shaft diameter $d_{sh} = 0.01$ m;

- Maximum operating temperature $= 70°C$;

The MR fluid used for prototype damper is MRF–132DG (Lord Corporation, USA Product). The properties of this MR fluid are presented in Fig.7:

From Fig.7, one can obtain the following parameter values:

- Shear rate: $\gamma^* = 1000s^{-1}$;
- Maximum magnetic field: $H = 250kA/m$;
- Off-state plastic viscosity: $\eta = 0.107Pa\text{-}s$;
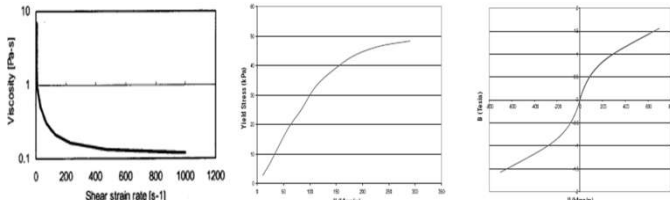- Yield stress: $\tau_y = 46.5kPa$;

Fig 7 Rheological properties of MRF–132DG

The design of MR fluid dampers assumes two main stages: 1) Hydraulic circuit design, and 2) Magnetic circuit design. Both stages presume an iterative calculus.

For the hydraulic circuit design the gap dimension g derives from condition of maximum dynamic range D.

The calculus relations for parameters in Eq. (44) are:

$$A_p = \frac{\pi \cdot \left[(d_{cyl} - 2g)^2 - d_{sh}^2 \right]}{4}; \tag{45}$$

$$w = \pi(d_{cyl} - g), \tag{46}$$

$$c = 2.07 + \frac{12 \cdot Q \cdot \eta}{12 \cdot Q \cdot \eta + 0.4 \cdot w \cdot g^2 \cdot \tau_y}; \tag{47}$$

$$Q = A_p \cdot v_p; \tag{48}$$

The rate of dynamic range D Vs gap dimension g is plotted in Fig.8 which gives $g = 0.001$ m for $D = 40$.

With these values we have determined the dimensional and functional parameters of hydraulic circuit:

$$w = 0.1225m, \; A_P = 1.05 \times 10^{-4} m^2,$$
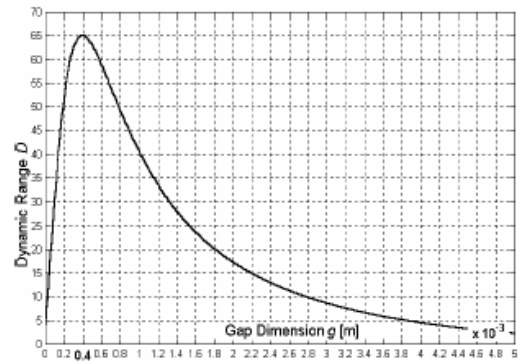
$$Q = 5.25 \times 10^{-5} m^3/s, c = 2.137,$$

Fig 8 Dynamic range D Vs. gap dimension g

$$\Delta P_\tau = 3.77 \times 10^6 Pa, \; \Delta P_\eta = 0.05 \times 10^6 Pa,$$
$$\lambda = 73, V_m = 49 \times 10^{-7} m^3,$$
$$\Delta P = 3.82 \times 10^6 Pa, F = \Delta P \cdot A_P = 4012N,$$
$$W_m = 198W, F_\tau = \Delta P_\tau \cdot A_P = 3959N.$$
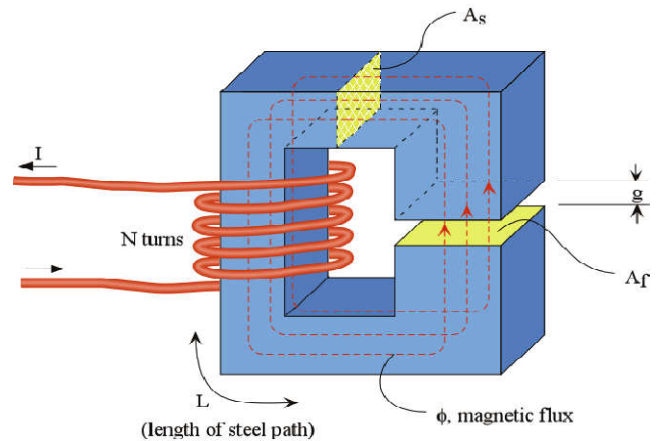
MR Damper Magnetic Circuit Design

Fig 9 Typical Magnetic circuit

For completeness, the description of the magnetic circuit design described in the Lord Corporation Engineering Note (1999b) is summarized in this section. The MR damper magnetic circuit typically uses low carbon steel , which has a high magnetic permeability and saturation, as a magnetic flux conduit to guide and focus magnetic flux into the fluid gap. Tasks in the design of a magnetic circuit are to determine necessary amp-turns (NI) for the magnetic circuit. An optimal design of the magnetic circuit requires to maximize magnetic field energy in the fluid gap while minimize the energy lost in steel flux conduit and regions of non-working areas. The total amount of steel in the magnetic circuit also needs to be minimized. However, sufficient cross-section of steel must be maintained such that the magnetic field intensity in the steel is very low.

The typical design process for a magnetic circuit is as follows:

1. Determine the magnetic induction B_f in the MR fluid to give desired yield stress τ_y (Fig.10 (a)).

For $\tau_y = 46.5kPa$, $B_f = 0.85T$.

2. Determine the magnetic field intensity H_f in the MR fluid (Fig.10 (b)).

For B_f =0.85T, H_f =250kA/m.

3. The total magnetic induction flux is given by $\Phi = B_f A_f$, where A_f is effective pole area including the fringe of magnetic flux. Because of the continuity of magnetic induction flux, the magnetic induction B_s in the steel is given by

$$B_s = \frac{\Phi}{A_s} = \frac{B_f \cdot A_f}{A_s} \qquad (49)$$

A_f =1.35×10^{-3} m², $A_S = 1.19 \times 10^{-3}$ m² and B_s =0.96T.

4. Determine the magnetic field intensity H_s in the steel using Fig.10(c).

For B_s =0.96T, H_s =0.46kA/m.

5. By using Kirchoffs's Law of magnetic circuits, the necessary number of amp-turns (NI) is

$$NI = \sum H_i L_i = H_f g + H_s L \qquad (50)$$
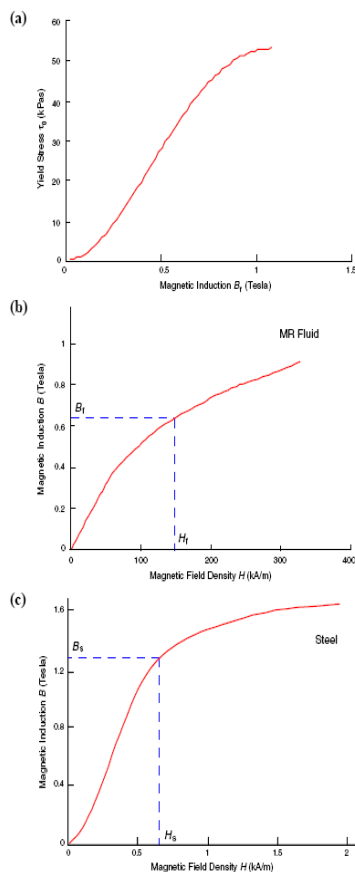

Fig 10 Basic Magnetic circuit design procedure (Engineering Note 1999b)

Where L= length of steel path which is equal to $L_s + L_c$ (Fig.11).

NI is calculated as 276 amp-turns. Taking I=2A, yields N=138.
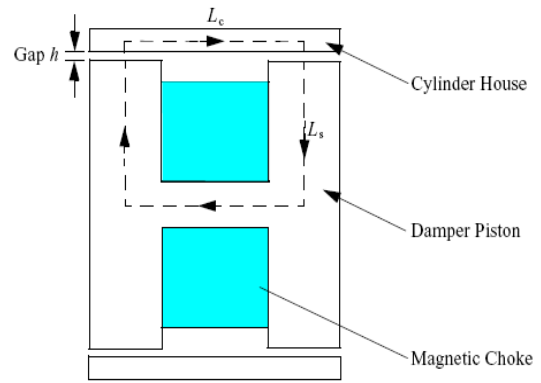

Fig 11 Magnetic Circuit of MR Damper

Other effects should also be considered during the circuit design process, such as non-linear magnetic properties of MR fluid and steel; possible losses at junctions and boundaries; limits on voltage, current, and inductance; possible inclusion of permanent magnet for fail-safe operation; and eddy currents.

The construction solution selected for proposed prototype MR fluid damper is presented in Fig.12, which is to be tested for its performance and compare with theoretical results.
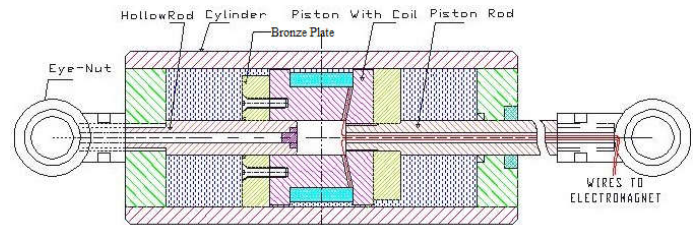

Fig 12 Prototype damper

CONCLUSIONS

In this work, a fundamental understanding of the dynamic behavior of Magnetorheological (MR) fluids has been developed through annular duct using Navier- Stokes equation based on the Herschel-Bulkley and Bingham models for Non-Newtonian fluid flows. These models are useful for further designing the MR Fluid Damper for structural vibration mitigation.

Commonly, the MRF damper piston does not remain in center during operation. This may be due to either manufacturer error or side loads due to inappropriate installation (which may result in non uniform temperature increases and local overheating, bearing malfunction and leakage, or scratching of the insulation and causing a short in the magnetic coil).

To overcome this problem, two end collars made up of bronze are installed on either side of proposed MR fluid damper shown in Fig.12. Moreover, bronze is softer than steel and will not scratch the cylinder surface.

References

1. M. Kciuk, S. Kciuk and R. Turczyn, Magnetorheological characterization of carbonyl iron based suspension, *Journal of Achievements in Materials and Manufacturing Engineering*, 2009: 33, pp.135-141.

2. Shinichi KAMIYAMA, Kazuo KOIKE and Zhi-ShanWANG, Rheological Characteristics of Magnetic

Fluids, JSME *International Journal*, 1987: 30 (263), pp.761-766.

3. Yukio Tomita, Flows of Non-Newtonian Fluids, JSME *International Journal*, 1987: 30 (270), pp.1877-1884.

4. N. Seetharamaiah AND G. Prasannakumar, Characterization Of Synthesized Magnetorheological (Mr) Fluids, Proceedings of The Second International Conference On Advances In Materials Processing And Characterisation, 2013: 2, PP.1027-1035.

5. Gheorghe GHITA, Marius GIUCLEA and Tudor Sireteanu, Modeling of Dynamic Behavior of Magnetorheological Fluid Damper by Genetic Algorithms Based Inverse Method, The 6th *International Conference on Hydraulic Machinery and Hydrodynamics, Timisoara, Romania*. 2004: pp.21-22.

****